Observation of Pedestal Plasma Turbulence on EAST Tokamak

2013 Plasma Sci. Technol. 15 732

(http://iopscience.iop.org/1009-0630/15/8/03)

Observation of Pedestal Plasma Turbulence on EAST Tokamak*

GAO Xiang (高翔), ZHANG Tao (张涛), HAN Xiang (韩翔),
ZHANG Shoubiao (张寿彪), WANG Yumin (王嵎民), LIU Zixi (刘子奚),
YANG Yao (杨曜), LIU Shaocheng (刘少承), SHI Nan (史楠),
LING Bili (凌必利), LI Jiangang (李建刚), and the EAST team

Institute of Plasma Physics, Chinese Academy of Sciences, Hefei 230031, China

Abstract Pedestal plasma turbulence was experimentally studied by microwave reflectometry on EAST tokamak. The characteristics of edge pedestal turbulence during dithering L-H transition, ELM-free H-mode phase and inter-ELM phase have recently been studied on EAST. An edge spatial structure of density fluctuation and its dithering temporal evolution is observed for the first time on the EAST tokamak during the L-H transition phase. A coherent mode usually appears during the ELM-free phase prior to the first ELM on EAST tokamak. The mode frequency gradually decreases as the pedestal evolves. Analysis shows that the coherent mode is in the pedestal region inside the separatrix. In plasma with type-III ELMs, a precursor mode before ELM is usually observed. The frequency of the precursor was initially about 150 kHz and gradually decreased till the next ELM. The mode amplitude increases or shows saturation before ELM. In the plasma with compound ELMs composed of high and low frequency ELMs, the precursor was also observed before the high frequency ELM while the harmonic oscillations with frequencies of 20 kHz, 40 kHz and 60 kHz appear before the low frequency ELM.

Keywords: H-mode, pedestal turbulence, reflectometry

PACS: *52.25.Os, 52.35.Hr, 52.55.Fa*

DOI: 10.1088/1009-0630/15/8/03

1 Introduction

The H-mode is characterized by a spontaneous formation of a transport barrier at the edge pedestal which is usually associated with repetitive edge localized modes (ELMs). It is believed that the confinement improvement in H-mode is due to the suppression or reduction of turbulent transport. There are clear experimental evidences for a fast reduction in the level of edge turbulence during L-H transition [1~5]. However, the L-H transition power threshold for the next step fusion device, e.g. ITER, is still uncertain since the physics involved in this transition process has not yet been fully understood [6]. The earliest theories attributed the transition to the increases in the radial electric field ($\mathbf{E}_\mathrm{r}$) [7~9] and its associated $\mathbf{E}_\mathrm{r} \times \mathbf{B}$ drift (mean flow) and thus turbulence suppression by the flow shear [10]. A more recent predator-prey model [11,12] reveals a complex interaction between zonal flows (ZFs), turbulence and the mean flow. When the ZFs are incorporated into a L-H transition model [12], the predator-prey-type competition between turbulence and ZFs will result in a limit cycle oscillation (LCO) phase where turbulent fluctuation level is modulated by a low frequency $\mathbf{E}_\mathrm{r}$ oscillation. The periodical modulation of flow and turbulence level preceding the L-H transition has been observed in ASDEX-Upgrade [13], DIII-D [14] and TJ-II stellarator [15] recently. On the EAST tokamak, a quasi-periodic $\mathbf{E}_\mathrm{r}$ oscillation with a frequency about 4 kHz and a modulation in edge turbulence preceding the L-H transition have been observed at marginal input power [16]. The oscillation amplitude, typically only of ∼3% in target D_α signal, is much smaller than those mentioned above. In the new campaign of EAST in 2012 spring, the previous water cooled graphite first wall was changed to molybdenum wall and an intermediate phase (labeled I phase) displaying dithering cycles with a much larger oscillating amplitude (∼30% in D_α signal) between L- and H-modes has been observed. Here, we call it dithering L-H transition. It is found that this dithering mainly occurs in plasmas with double null (DN) and upper single null (USN) configurations [17].

The H-mode pedestal plays a central role in achieving high performance plasma [18]. The transport analyses in Refs. [19,20] have shown that the ion thermal transport coefficient in the edge pedestal region was close to the neoclassical value while the electron thermal transport level was still higher than that predicted by the neoclassical theory. This result suggests that there is remnant turbulence in the pedestal region. In addition, the experimental results on DIII-D [21,22] and ASDEX Upgrade [23] showed that the pressure gradient in the edge pedestal recovered in a short time after an ELM crash and then saturated for a long time up to the next ELM crash. Electromagnetic turbulence, such as the

*supported by the National Magnetic Confinement Fusion Program of China (Nos. 2010GB106000, 2010GB106001) and National Natural Science Foundation of China (Nos. 11021565, 11275234)

kinetic ballooning mode [24,25], has been suggested to be the responsible mechanism for this saturation of the pedestal pressure gradient [22]. These results indicate that the turbulence may play an important role in the pedestal transport process.

An X-mode microwave reflectometer operating in the V-band frequency (50∼75 GHz) range has been developed for the measurement of density fluctuation on EAST tokamak. In this paper, we present the turbulence characteristics measured by the reflectometry during the dithering L-H transition, ELM-free and inter-ELM phases. In section 2, the experimental setup is briefly described. The experimental results are presented in section 3 and a summary is given in section 4.

2 Experimental setup

The EAST tokamak is a non-circular full superconducting tokamak with a major radius (R) of 1.75 m and a minor radius (a) of 0.45 m. It was designed for steady state divertor operation for a duration of 1000 s. The device can operate in multi-configurations including single null (SN) divertor, double-null (DN) divertor or circular configuration with a limiter. The H-mode was achieved on EAST tokamak in 2010 [26] and the confinement during ELMy H-mode has been studied [27]. In the 2012 spring campaign, the material for first wall has been changed from graphite to molybdenum besides the graphite divertors, as shown in Fig. 1(a). All the discharges presented in this paper are from this campaign and operate with working gas of deuterium, at plasma current (I_p) from -400 kA to -500 kA and toroidal magnetic field (B_t at $R = 1.75$ m) of -1.9 T. Here, the minus sign of I_p and B_t indicate that both quantities are anticlockwise viewed from the top of the device. Therefore, the ion $\mathbf{B}\times\nabla\mathbf{B}$ drift direction is towards the X-point in the USN configuration, i.e. so called 'favorable' direction, while this drift direction is away from the X-point in the lower single null (LSN) configuration, i.e. 'unfavorable' direction. The H-mode is achieved by applying the lower hybrid wave (LHW) and ion cyclotron resonance heating (ICRH) after wall conditioning by lithium (Li) evaporation after the plasma breakdown and the real-time injection of fine Li powder into the plasma edge.

The schematic of the reflectometry on EAST is shown in Fig. 1(b). The microwave source is a low noise frequency synthesizer with operating frequency ranging from 2 GHz to 20 GHz. By using a power provider, the output wave of synthesizer is split into two portions, one for probing the plasma and the other for reference. To achieve heterodyne detection, the probing wave frequency is modulated in a single sideband modulator (SSBM) by a quartz oscillator at 100 MHz. The wave frequency output from SSBM is upshift 100 MHz and then translated into the V-band frequency range by an active quadrupler. Two adjacent antennae, located at the equatorial plane of the low field side on EAST, are used for emission and reception. After the qaudrupling of its frequency, the reference wave is mixed with the reflected wave from the plasma. An I/Q detector is used to measure the in-phase and 90°-phase signal to allow absolute phase and amplitude detection. The V-band circuit shown in Fig. 1(b) is also used for the density profile measurement by changing the microwave source from the synthesizer to a voltage controlled oscillator (VCO) in experiments [28]. As a result, the density profile and density fluctuation can not be simultaneously measured by the reflectometry. When the reflectomety is used for density fluctuation measurement, the operating frequency band is from 50 GHz to 75 GHz and the frequency of the probing wave can be fixed or changed step by step. The wavenumber of the turbulence measured by the reflectometry is $k_\perp \approx 0 \sim 3$ cm^{-1}, corresponding to $k_\perp \rho_\mathrm{s} \approx 0 \sim 0.4$.

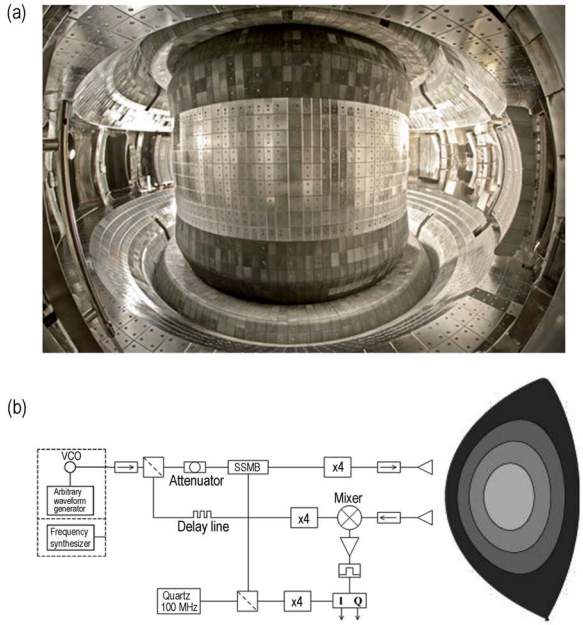

Fig.1 (a) EAST superconducting tokamak, (b) Schematic of X-mode reflectometry for density fluctuation measurement on EAST tokamak

3 Experimental results

3.1 Turbulence behavior during dithering L-H transition

Fig. 2 shows time evolution of discharge parameters for EAST shot 40846 which operated in the DN configuration. The plasma is heated by 1.2 MW LHW and 0.5 MW ICRH. The H-mode is achieved at about 2.733 s. Before 2.717 s the D_α signal is initially at a reduced level compared with L-mode and then gradually increases. The diamagnetic energy (W_dia) and core line averaged density ($< n_\mathrm{e} >$) show gradually increase after 2.733 s. An intermediate phase (labeled as I phase) with D_α showing dithering cycles or oscillation is observed between 2.717 s and 2.733 s, as shown

in Fig. 2(d). Following the I phase, the plasma stays in ELM-free H-mode up to the appearance of type-III ELM at about 3 s.

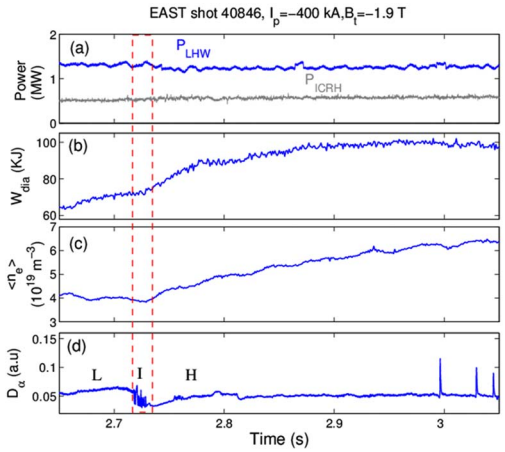

Fig.2 Evolution of parameters for EAST shot 40846. (a) Heating powers of LHW ($P_{\rm LHW}$) and ICRH ($P_{\rm ICRH}$), (b) Diamagnetic energy $W_{\rm dia}$, (c) Core line averaged density $< n_{\rm e} >$, (d) D_α signal. 'L', 'I' and 'H' indicate the L-mode phase, the intermediate phase and the H-mode phase, respectively. The rectangular indicates the I phase (color online)

During the dithering L-H transition, edge density fluctuation has been measured by reflectometry. Fig. 3(a) shows the expanded D_α signal covering the L, I and H phase and Fig. 3(b) shows the spectrogram of the complex wave amplitude (S) measured by the X-mode reflectometry with probing frequency of 60 GHz, corresponding to the cutoff at a normalized radius (ρ) of about 0.95. Here, S is constructed from the in-phase and 90°-phase signal measured by the I/Q detector. It can be seen that the spectrum of S also shows oscillatory feature in the I phase: when the D_α signal decreases, the high frequency components in fluctuation spectrum of S are suppressed and fluctuation energy converges to zero frequency while a broad spectrum similar to L-mode forms when the D_α signal recovers (Fig. 3(d)). Therefore, the relative density fluctuation level ($\delta n/n$) shown in Fig. 3(c) also shows oscillations during the I phase: the $\delta n/n$ decreases when D_α signal is reduced while the $\delta n/n$ recovers to L-mode level when D_α signal increases again. This observation is very similar to those observed on ASDEX-Upgrade [13] and DIII-D [14] by Doppler reflectometry where the density fluctuation oscillation is explained by a predator-prey type competition between background turbulence and ZFs [11]. Further analysis has shown that this oscillation of fluctuation level during the I phase only occurs about 2 cm inside the separatrix [17]. It is also observed that the $\delta n/n$ stays at a low level from the time the H-mode appears (2.733 s) up to about 2.74 s. The decrease of edge turbulence could result in a reduction of turbulent transport and lead to the improvement of plasma confinement. This low fluctuation level phase after L-H transition was also observed in other devices [1~5]. The increase of $\delta n/n$ after 2.74 s is due to the appearance of a coherent mode as indicated in Fig. 3(b). The detail of this mode is presented in the following subsection.

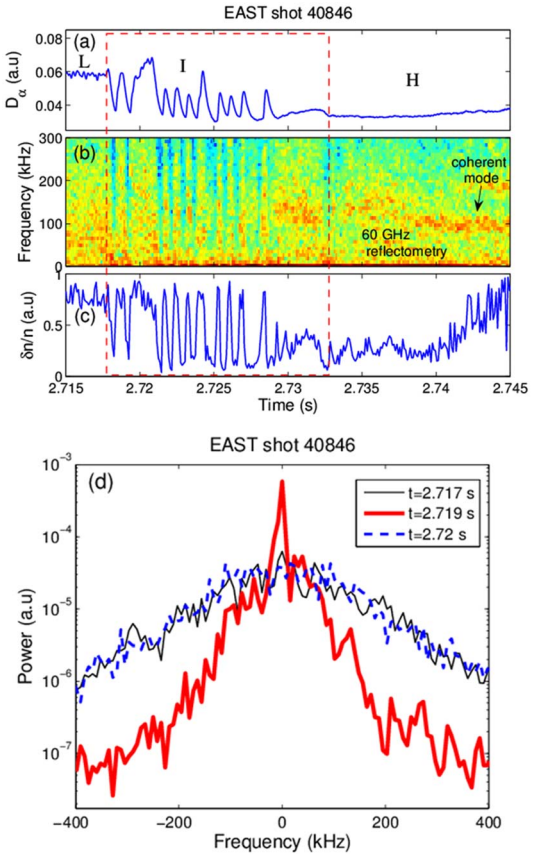

Fig.3 Dithering L-H transition. (a) D_α signal, (b) Spectrogram of complex signal measured by 60 GHz reflectometry, (c) Estimated relative density fluctuation level $\delta n/n$ and (d) Spectra at three different time (color online)

3.2 Coherent mode during the ELM-free phase

Fig. 4 shows the plasma parameters for EAST shot 41713 which operated in LSN configuration and was heated by 1.2 MW LHW and 0.6 MW ICRH. The L-H transition occurs at about 3.28 s after which the D_α signal shows an abrupt reduction and both $W_{\rm dia}$ and $< n_{\rm e} >$ begin to increase. No dithering between the L- and H-mode is observed in this LSN plasma. A coherent mode with a frequency of about 100 kHz appears in the density fluctuation spectrum (Fig. 4(e)) measured by a 54 GHz reflectometry at about 3.3 s. The mode frequency gradually decreases as the pedestal evolves while the mode amplitude shows no clear change (Fig. 4(f)). This mode disappears at last or is buried in the broad band fluctuation. This coherent mode can not be observed in the magnetic fluctuation spectrum measured by edge fast magnetic probe even when the probe is inserted inside the separatrix of plasma. This mode has been commonly observed in plasmas heated by LHW+ICRH, LHW or ICRH and also in plasmas with DN, LSN or USN configurations on EAST.

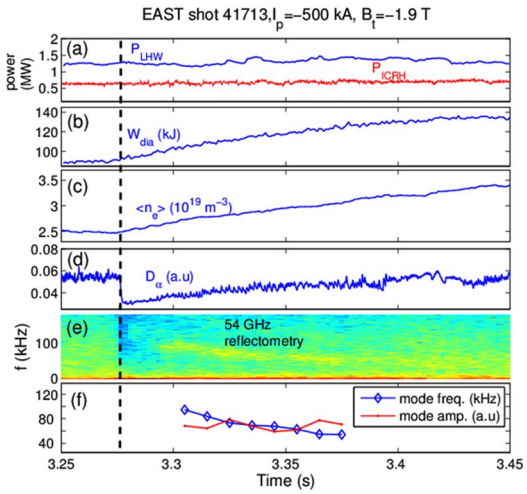

Fig.4 Evolution of parameters for EAST shot 41713. (a) Heating powers of $P_{\rm LHW}$ and $P_{\rm ICRH}$, (b) $W_{\rm dia}$, (c) $< n_{\rm e} >$, (d) $\rm D_\alpha$ signal, (e) Spectrogram measured by 54 GHz reflectometry and (f) The coherent mode frequency and amplitude (color online)

In order to confirm the localization of this coherent mode, an experiment has been done by changing the reflectometry frequency shot by shot in a series discharges with similar plasma parameters. The plasma density before L-H transition in these shots is $< n_{\rm e} >= 2 \times 10^{19}$ m^{-3}. All these shots operate in DN configuration. Eight probing frequencies, i.e. 52 GHz, 54 GHz, 56 GHz, 58 GHz, 60 GHz, 64 GHz, 68 GHz and 72 GHz, are selected for the density fluctuation measurement. Fig. 5 shows the divertor $\rm D_\alpha$ as references and the fluctuation spectra measured by reflectometry with 52 GHz, 56 GHz, 60 GHz, 64 GHz and 72 GHz. In these plots, we have taken the occurrence time of I phase ($t_{\rm LI}$) as time reference. The coherent mode can be clearly seen in the spectra measured by 52 GHz∼60 GHz reflectometry (including 54 GHz and 58 GHz, not shown here) while the 68 GHz and 72 GHz reflectometry can not see the mode, for which broad band fluctuation spectra dominate. For 64 GHz reflectometry, the mode can be seen but buried in the broadband fluctuation. Although the starting time of the mode is different, the mode generally disappears before $t - t_{\rm LI} = 0.06$ s in these similar discharges. Due to the fact mentioned above that the reflectometry can not simultaneously measure the density profile and fluctuation, a similar discharge, shot 41554, with the same density is selected to study the localization of the coherent mode. Fig. 6 shows the density profiles measured by reflectometry at two different time slices ($t - t_{\rm LI} = 0.026$ s and 0.055 s) after the access of H-mode, and the cutoffs of the reflectometry with the eight probing frequencies are also indicated in each profile. It can be seen that the 68 GHz and 72 GHz reflectometry measures the density fluctuation in core region while 52∼60 GHz reflectometry does in the pedestal region. For 64 GHz refletometry, the cutoff is just around the point which connects the core and the pedestal. This may be the reason why the 64 GHz reflectometry can see both the coherent

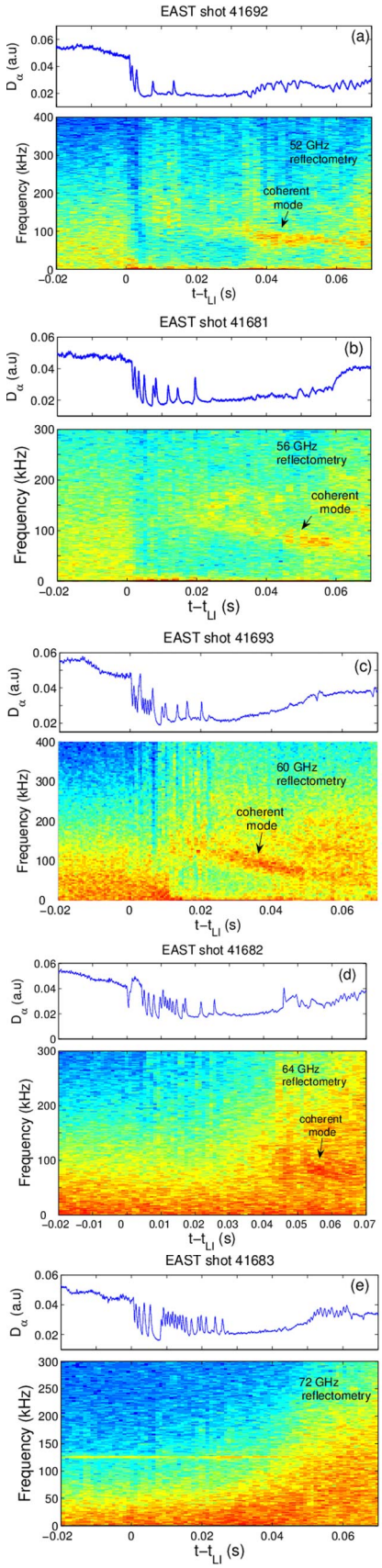

Fig.5 Density fluctuation measurement by reflectometry with different probing frequencies. The upper plots in (a)∼(e) show the divertor $\rm D_\alpha$ signals and the lower plots show the spectrogram of density fluctuation. $t_{\rm LI}$, the transition time from L-mode to I phase, is taken as time reference (color online)

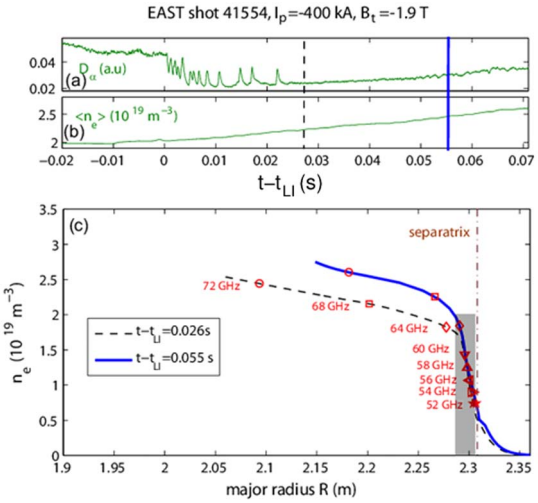

Fig.6 Localization analysis of coherent mode using EAST shot 41554: (a) D_α signal, (b) $<n_e>$, and (c) Density profiles at two time slices after the access of H-mode. The shaded rectangular indicates the available region of the coherent mode deduced from reflectometry measurement (color online)

mode and the broad band fluctuation in Fig. 5(d). Therefore, we conclude that the coherent mode observed in the ELM free phase is in the pedestal region.

The characteristics of the coherent mode observed here are similar to the quasi coherent modes (QCMs) observed in the enhanced D_α (EDA) H-mode on Alcator C-Mod [29], e.g. the sweeping down in frequency and localization in edge pedestal. However, the differences between them are evident. The most significant difference is that the QCMs in EDA H-mode can enhance the pedestal particle transport and decrease the rate of, or even cease the density rise while the coherent mode on EAST shows no clear influence on the density or energy rise (Fig. 4). In addition, the QCMs have clear magnetic fluctuation while the coherent mode here can not be observed by magnetic probe.

3.3 Characteristics of pedestal turbulence during the inter-ELM phase

H-mode plasma on EAST is usually associated with type-III ELMs. It is a common observation that a precursor mode appears before this type-III ELM. Fig. 7 shows a typical plasma with type-III ELMs which have a frequency ($f_{\rm ELM}$) of about 200 Hz and produce small relative energy loss $\Delta W_{\rm ELM}/W_{\rm dia}$ less than 1%. Fig. 7(c) shows the density fluctuation spectrogram measured by a 52 GHz reflectometry with cutoff in the pedestal region. The precursor mode with a born frequency of ~150 Hz appears about 1 ms after ELM crash and the mode frequency gradually decreases till the next ELM. The fluctuation power integrated from 50 kHz and 200 kHz as shown in Fig. 7(d) indicates that the mode amplitude gradually increases or saturates before the ELM. This precursor is not observed in the magnetic fluctuation measured by the edge fast magnetic probe.

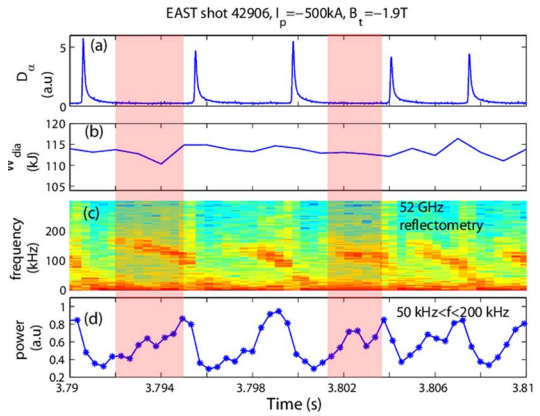

Fig.7 EAST shot 42906 with type-III ELM: (a) D_α signal, (b) $W_{\rm dia}$, (c) Spectrogram of density fluctuation measured by 52 GHz reflectometry and (d) The fluctuation power integrated from 50 kHz to 200 kHz (color online)

Compound ELM is also observed on EAST H-mode plasma as shown in Fig. 8 for shot 42902. The ELMs in this shot are composed of 200 Hz and 70 Hz ELMs while both ELMs lead to small energy loss $\Delta W_{\rm ELM}/W_{\rm dia}$ <1%. The precursor mode is also observed before the 200 Hz ELM in density fluctuation spectrogram measured by a 64 GHz reflectometry with cutoff in pedestal. However, this high frequency precursor is not observed before the 70 Hz ELM. Instead, harmonic oscillations (HOs) with frequency of ~20 kHz, 40 kHz and 60 kHz are clearly observed before the 70 Hz ELM in magnetic fluctuation. The density fluctuation also captures part of the HOs, as indicated in Fig. 8(c). The toroidal mode number n of the HOs are -1, -2 and -3, respectively, which are obtained by making a time-windowed Fourier decomposition of the signals of a toroidal set of magnetic probes and analyzing the relative phase shift of the fluctuations. Here, the minus n means that the mode rotates in the electron diamagnetic direction (EDD). The measurement of core CXRS shows that the core toroidal rotation is

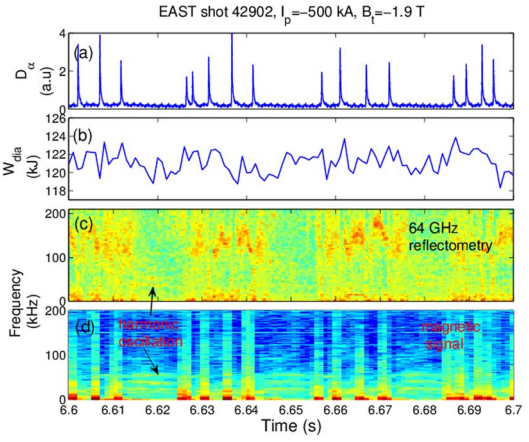

Fig.8 EAST shot 42902 with compound ELM: (a) D_α signal, (b) $W_{\rm dia}$, (c) Spectrogram of density fluctuation measured by 64 GHz reflectometry and (d) Spectrogram of magnetic fluctuations measured by edge magnetic probes (color online)

in the ion diamagnetic direction (IDD). Therefore, the HOs rotating in EDD should originate in the edge. Similar mode was also observed in other devices, e.g. the edge harmonic oscillations (EHOs) in QH mode on DIII-D [30]. It was shown that the EHOs can lead to increased particle transport and reduced edge density and density gradient, and thus holds the edge pressure gradient and the edge bootstrap current below the ELM instability limit [31]. It is conjectured that the HOs observed on EAST can induce particle or heat transport in pedestal, slower the pedestal evolution and postpone the appearance of the ELM. This conjecture needs confirmation in future.

4 Summary

In summary, the characteristics of edge pedestal turbulence during dithering L-H transition, ELM-free and inter-ELM phase on EAST have been presented. The density fluctuation measured by reflectometry at the edge shows an oscillation in the I phase between L- and H-mode while the core density fluctuation shows no oscillation. During the ELM-free phase after L-H transition but before the first ELM, a coherent mode with an initial frequency about 100 kHz appears and the mode frequency decreases gradually. The mode disappears at last and is replaced by broad band fluctuation. Analysis shows that the mode localizes in pedestal region just inside the separatrix. A precursor mode (about 150 kHz) is usually observed prior to type-III ELM in density fluctuation while it is not observed in magnetic fluctuation measured by edge magnetic probes. In a plasma with compound ELMs, the precursor mode is also observed before the high frequency ELM while harmonic oscillations with frequency of 20 kHz, 40 kHz and 60 kHz and respective toroidal mode number $n = -1$, -2 and -3, replacing the precursor mode, appear before the low frequency ELM. The conjecture that the harmonic oscillations can induce transport in pedestal and postpone the appearance of ELMs needs further confirmation. In the future, the relation between pedestal turbulence and pedestal parameter evolution and pedestal transport will be studied using new and improved diagnostics on EAST.

References

1 Burell K H, Carlstrom T N, Doyle E J, et al. 1990, Phys. Fluids B, 2: 1405
2 Doyle E J, Groebner R J, Burell K H, et al. 1991, Phys. Fluids B, 3: 2300
3 Rettig C L, Peebles W A, Burell K H, et al. 1993, Nucl. Fusion, 33: 643
4 Tynan G R, Schmitz L, Blush L, et al. 1994, Phys. Plasmas, 1: 3301
5 Moyer R A, Burell K H, Carlstrom T N, et al. 1995, Phys. Plasmas, 2: 2397
6 Wagner F. 2007, Plasma Phys. Control. Fusion, 49: B1
7 Itoh S I and Itoh K. 1988, Phys. Rev. Lett., 60: 2276
8 Shaing K C and Jr. Crume E C. 1989, Phys. Rev. Lett., 63: 2369
9 Hassam A B, Antonsen T M, Jr. Drake J F, et al. 1991, Phys. Rev. Lett., 66: 309
10 Biglari H, Diamond P H, and Terry P W. 1990, Phys. Fluids B, 2: 1
11 Kim E J and Diamond P H. 2003, Phys. Rev. Lett., 90: 185006
12 Kim E J and Diamond P H. 2003, Phys. Plasmas, 10: 1698
13 Conway G D, Angioni C, Ryter F, et al. 2011, Phys. Rev. Lett., 106: 065001
14 Schmitz L, Zeng L, Rhodes T L, et al. 2012, Phys. Rev. Lett., 108: 155002
15 Estrada T, Hidalgo C, Happel T, et al. 2011, Phys. Rev. Lett., 107: 245004
16 Xu G S, Wan B N, Wang H Q, et al. 2011, Phys. Rev. Lett., 107: 125001
17 Zhang T, Gao X, Zhang S B, et al. 2013, Phys. Lett. A, 377: 1725
18 Doyle E J, Houlberg W A, Kamada Y, et al. 2007, Nucl. Fusion, 47: S18
19 Stacey W M. 2004, Phys. Plasmas, 11: 1511
20 Callen J D, Groebner R J, Osborne T H, et al. 2010, Nucl. Fusion, 50: 064004
21 Groebner R J, Osborne T H, Leonard A W, et al. 2009, Nucl. Fusion, 49: 045013
22 Groebner R J, Snyder P B, Osborne T H, et al. 2010, Nucl. Fusion, 50: 064002
23 Burckhart A, Wolfrum E, Fischer R, et al. 2010, Plasma Phys. Control. Fusion, 52: 105010
24 Snyder P B, Groebner R J, Leonard A W, et al. 2009, Phys. Plasmas. 16: 056118
25 Yan Z, McKee G R, Groebner R J, et al. 2011, Phys. Rev. Lett., 107: 055004
26 Xu G S, Wan B N, Li J G, et al. 2011, Nucl. Fusion, 51: 072001
27 Liu Z X, Gao X, Zhang W Y, et al. 2012, Plasma Phys. Control. Fusion, 54: 085005
28 Zhang S B, Gao X, Ling B L, et al. 2013, accepted as publication in Plasma Sci. Technol.
29 Mazurenko A, Porkolab M, Mossessian D, et al. 2002, Phys. Rev. Lett., 89: 225004
30 Greenfield C M, Brullel K H, DeBoo J C, et al. 2001, Phys. Rev. Lett., 86: 4544
31 Burrel K H, Osborne T H, Synder P B, et al. 2009, Nucl. Fusion, 49: 085024

(Manuscript received 28 April 2013)
(Manuscript accepted 4 June 2013)
E-mail address of GAO Xiang: xgao@ipp.ac.cn